

У статті запропоновано використовувати в порожнистій серцевині оптичного гіроскопу фотонно-кристалічне волокно 1550 нм, Ø10 мкм замість звичайних волокон. Фотонні кристали мають спеціальні властивості та можливості, які призводять до величезного потенціалу для додатків зондування. Запропоновані рішення дозволять усунути багато проблем, що існують у звичайному волоконно-оптичному гіроскопі, і отримати більш точні результати при тих же умовах при використанні фотонно-кристалічного волокна

Ключові слова: оптичний гіроскоп, ефект Саньяка, фотонно-кристалічне волокно

В статье предложено использовать в полой сердцевине оптического гироскопа фотонно-кристаллическое волокно 1550 нм, Ø10 мкм вместо обычных волокон. Фотонные кристаллы обладают специальными свойствами и возможностями, которые приводят к огромному потенциалу для приложений зондирования. Предложенные решения позволяют устранить много проблем, существующих в обычном волоконно-оптическом гироскопе, и получить более точные результаты при тех же условиях при использовании фотонно-кристаллического волокна

Ключевые слова: оптический гироскоп, эффект Саньяка, фотонно-кристаллическое волокно

UDC 621.373.826

DOI: 10.15587/1729-4061.2015.39203

THE ADVANTAGES OF USING PHOTONIC CRYSTAL FIBERS INSTEAD OF THE CONVENTIONAL FIBERS IN OPTICAL GYROSCOPE

Haider Ali Muse

Postgraduate student

Faculty of electronic engineering

Department of Physical Foundations

of Electronic Engineering

Kharkiv national university

of radio electronics

Lenina ave., 14, Kharkov, Ukraine, 61000

E-mail: Hadr_2005@yahoo.com

1. Introduction

In recent years, photonics has become an attractive alternative to electronics technology due to the advantages of information processing in optical domain. On-chip and chip-to-chip optical interconnects offer a solution to this problem and promise a higher bandwidth to keep pace with transistors while lowering power consumption and being immune to EMI. On the other hand, the realization of optical interconnects requires the development of high-speed modulation and low power light sources, optical switches, waveguides and their compact integration. Photonic crystal is one of the most promising platforms for optical information processing as it can enable compact and efficient photonic devices and also their large scale integration. These are structures with periodic dielectric modulation on the order of the wavelength of light. Fiber optic gyroscopes (FOG) are solid-state rotation sensors that are appropriate for a wide variety of application. High performance, long-lifetime gyroscope applications, such as satellite pointing, was formerly the domain of spinning wheel gyroscopes. Recently, the fiber optic gyroscope (FOG) has reached performance levels that make this solid-state rotation sensor appropriate for applications like these. At the same time demand are (fiber optical gyroscope) in a wide range of characteristics of accuracy – 10.0 deg/h to 0, 001 deg/hr. In Russia, the leader in the production of a number of FOG accuracy class 10.0–1.0 deg/h is LLC “Physoptic”. However, there is a gap from the foreign systems generally recognized as FOG for the control and navigation systems moving objects of various kinds level in FOG navigational accuracy class

(0.01–0.001 deg/h). Performance characteristics of fiber-optic gyroscope increased accuracy are largely dependent on the characteristics of its basic elements and features of its assembly techniques. Thus, the development of fiber-optic gyroscope and methods of its production is an urgent task. Due to their unique geometric structure, photonic crystal fibers present special properties and capabilities that lead to an outstanding potential for sensing applications.

2. Analysis of published data and problem statement

The performance characteristics of fiber-optic gyroscope, increased accuracy is largely dependent on the characteristics of its basic elements and features of its assembly techniques. Thus, the development of fiber-optic gyroscope and methods of its production is an urgent task. The diversity of unusual features of photonic crystal fibers, beyond what conventional fibers can offer, leads to an increase of possibilities for new and improved sensors. There is a huge interest of the scientific community in this original technology for applications in a variety of fields. Thanks to the flexibility for the cross section design, photonic crystal fibers (PCFs) [1, 2] have achieved excellent properties in birefringence [3, 4], dispersion [5, 6], single polarization single mode [7, 8], nonlinearity [9], and effective mode area [10, 11], and also excellent performances in the applications of fiber sensors [12, 13], fiber lasers [14, 15] and nonlinear optics [16, 17] over the past several years. Large numbers of research papers have highlighted some optical properties of the PCFs such as ultrahigh birefringence and unique chromatic dispersion,

which are almost impossible for the conventional optical fibers. The aim of this work was to conduct theoretical studies of the conditions of use of photonic crystal fiber (PCF) as a instead of the fiber optical gyroscope.

With the development of optoelectronic technology [18], optical fibers have been intensively investigated at various sensor fields owing to their unique characteristics such as multiplexing, remote sensing, high flexibility, low propagating loss, high sensitivity, low fabrication cost, small form factor, high accuracy, simultaneous sensing ability, and immunity to electromagnetic interference. This is the case of Photonic Crystal Fibers (PCFs), also called holey fibers, which contain arrays of tiny air holes along their structure and allow, among other new applications, the fabrication of new optical fiber sensors. A few years later, in 1991, Yablonovitch and co-workers produced the first photonic crystal by mechanically drilling holes a millimeter in diameter into a block of material with a refractive index of 3.6 [19]. In 1995 Birks et al. proposed a fiber with air holes along its length that could guide light through this structure with interesting properties [20, 21]. Nowadays the PCF has become a subject of extensive research and has opened a new range of possible applications. The structure of the PCF enables to have different types of fibers such as endless single mode, double clad, germanium or rare earth doped, high birefringence, and many others with particular features due to its manufacturing flexibility. This variety of choices permits the use of PCF in numerous applications such as sensors which measure physical parameters (temperature, pressure, force, etc.), chemical compounds in gas and liquids, and even biosensors [22, 23].

3. The purpose and objectives of the study

The following tasks were solved to reach the work purpose:

1. For hollow core fibers to realize their potential and advantages over conventional fibers in fiber optic gyroscopes. Long fiber lengths in a PCFG generally offer improved measurement sensitivity. The current loss levels of hollow core fibers designed for single mode transmission limit the fiber length. Although most of the light propagates in air, the portion that interacts with the silica hollow core wall experiences scattering and other loss mechanisms due to imperfections at this boundary.

2. The hollow core fibers described herein were designed with geometries for glass and coating diameter similar to conventional telecommunication fibers. For PCFG applications, coiling many turns of fiber benefits from a reduced diameter fiber, such as one with an 80 micron glass diameter, which is typical for many PCFGs. The hollow core fibers offer improved bend sensitivity allowing for tighter coils, but require a redesign of the fiber diameter to further reduce the space occupied by the fiber on the coil. This will require design and development activity to ensure that the reduced size will not compromise the optical performance produced by the special core and cladding bandgap regions.

3. The hollow core fiber offers a low reflectance interface, offering improved stability. Where designs require an alternative interface, such as a splice, mechanical coupling, or other type, reflections and mechanical integrity of the interface will need to be managed.

4. Fiber optical gyroscope

Fiber optical gyroscope is based on the Sagnac effect [24]. Sagnac effect generates an optical phase difference, $\Delta\phi$, between two counter propagating waves in a rotating fiber coil (optical path) [25]:

$$\Delta\phi = \frac{8\pi S}{\lambda c} \Omega, \tag{1}$$

where ($\Delta\phi$) – phase difference, Ω – angular velocity, C – light -/signal velocity, λ – wavelength, S – is the scale factor

Fig. 1 shows fibers optic gyroscope as the simplest rotation sensors. They are widely used in commercial applications where their dynamic range and linearity limitations are not constraining.

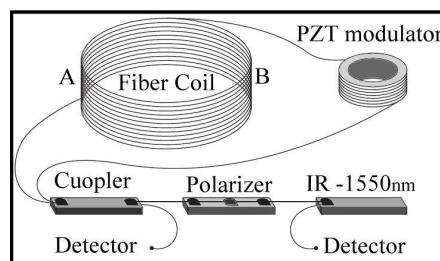


Fig. 1. Scheme of fiber optic gyroscope

During the rotation of angular velocity contour (Ω), an apparent distance between points A and B for the oppositely traveling beams changes. For a wave traveling from point A to point B, i.e., in a direction similar to the direction of rotation of the contour, the distance is extended, as in a time dt point B moves to the angle ($d\phi = \Omega \cdot dt$). This is for lengthening the path of the light beam is equal to $v \cdot dt$, since at each instant the beam is directed at a tangent to the contour at that same tangential linear velocity directed projection ($\vec{v} = v \cdot \cos\alpha = \Omega \cdot r \cdot \cos\alpha$). Thus, the length of the path traversed by the beam is equal to $Dl + v \cdot dt$. Arguing similarly, for opposing traveling light beam will be a reduction in the apparent path segment $Dl - v \cdot dt$. Considering the speed of light invariant quantity, apparent elongation and reduction paths for opposing beams can be considered equivalent to extensions and contractions of time intervals, i. e.,

$$\Delta t_1 = \frac{1}{c} (\Delta l + v \cdot dt), \tag{2}$$

$$\Delta t_2 = \frac{1}{c} (\Delta l - v \cdot dt). \tag{3}$$

If the relative time delay of counter propagating waves occurring during the rotation, expressed in terms of the phase difference of counters propagating waves, it will be

$$\begin{aligned} \Delta\phi &= \omega \cdot \Delta\tau = \frac{4 \cdot \omega \cdot S}{c^2} \cdot \Omega = \\ &= \frac{8 \cdot \pi \cdot v \cdot S}{c^2} \cdot \Omega = \frac{8 \cdot \pi \cdot S}{\lambda \cdot c}, \end{aligned} \tag{4}$$

where $\omega = 2 \cdot \pi \cdot \nu$,

$$\lambda = \frac{C}{\nu}$$

In the fiber optic gyroscope, an optical fiber is used as the medium of propagation for the IR 1550 nmλ. A long fiber cable is wound into loops in order to increase the effective area of the system. Two beams are again propagating through the fiber in opposite directions. Due to the Sagnac effect, the beam travelling against the rotation experiences a slightly shorter path delay than the other beam. Since the optical radiation propagates in a material medium, and it refers to the optical fiber, which is made of quartz or quartz glass, such physical phenomena as the birefringence effect, Kerr effect, Faraday effect, etc. Adversely affect the angle of rotation loop fiber optic gyroscopes and registered phase of the optical signal. These effects associated with the process of optical radiation propagation in the material of the optical medium, leading to a phase shift of counter propagating waves, which is not associated with the rotation of the closed loop. The negative effects are also associated with the processes of scattering and reflection of light in an optical path, the polarization non-reciprocity effect associated with the asymmetric arrangement of anisotropic elements, relative to the centre of the fiber loop, or anisotropic fiber properties. This problem was solved, and solved by the use of frequency and phase modulation of the optical radiation is used, which allows to shift the zero point on the slope with the maximum slope of the interference signal. The resulting differential phase shift is measured through interferometry, thus translating one component of the angular velocity into a shift of the interference pattern which is measured photometrically.

5. Hollow-core photonic crystal fibres (HC-PCFs)

Hollow-core photonic crystal fibers are optical fibers with claddings made of glass incorporating arrays of air holes. The core is formed by omitting several unit cells of material from the cladding. The “holey” cladding has a two dimensional photonic bandgap that can confine light to the core for wavelengths around a minimum-loss wavelength λ_c, even when the core is hollow and filled with air [26, 27]. In contrast, a conventional fiber guides light by total internal reflection so its core must have a higher refractive index than the cladding. Usually, this preform is then first drawn to a cane with a diameter of e. g. 1 mm, and thereafter into a fiber with the final diameter of e. g. 125 μm. Particularly soft glasses and polymers (plastics) also allow the fabrication of preforms for photonic crystal fibers by extrusion [28, 29]. There is a great variety of hole arrangements, leading to PCFs with very different properties. All these PCFs can be considered as specialty fibers. In this paper used the fibers of the type Hollow Core photonic crystal fiber, 1550 nm, Ø10 μm, core Hollow core Photonic Bandgap Fibers guide light in a hollow core, surrounded by a microstructured cladding of air holes and silica. Fig. 2 illustrated Typical attenuation and dispersion.

If the transverse scale of Hollow-core photonic crystal fibers changes without otherwise changing the structure of fibers, the wavelength λ_c of minimum attenuation must scale in proportion [30]. Without recourse to the approximations of the previous section, the mean square amplitude of the roughness component that couples light into modes with effective indices between n and n+δn is

$$u^2 = \frac{k_B T}{4\pi\gamma(n-n_0)} \coth\left(\frac{(n-n_0)kW}{2}\right) \delta n, \tag{5}$$

where γ – the surface tension; k_B – Boltzmann’s constant; T – the temperature.

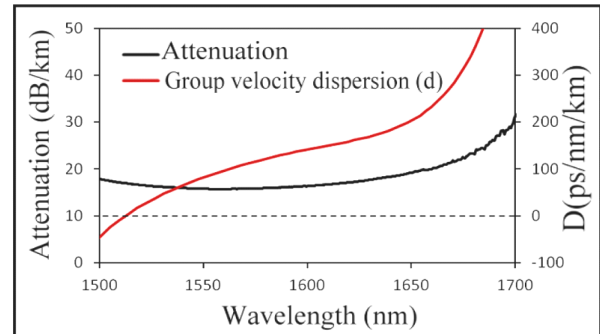


Fig. 2. Typical attenuation and dispersion

The attenuation to these modes is proportional to u² [31] but the only other independent length scale it can vary with is λ_c. As attenuation has units of inverse length, it must therefore by dimensional analysis be inversely proportional to the cube of λ_c. If this is true for every set of destination modes, it must be true for the net attenuation α to all destination modes, so

$$\alpha(\lambda_c) \approx \frac{1}{\lambda_c^3}. \tag{6}$$

This equation (described phenomenologically in [27] but without theoretical support) predicts the attenuation of a given fiber drawn to operate at different wavelengths. The result differs from the familiar 1/λ⁴ dependence of Rayleigh scattering in bulk media [32], and importantly applies to inhomogeneities at all length scales not just those small compared to λ. We measured attenuation spectra by the cut-back technique. A cut-back length of at least 50 m allowed transient leaky modes to decay away, so that only the fundamental mode is measured. For a set of similar Hollow-core photonic crystal fibers we determined the minimum attenuation as a function of the wavelength λ_c of the minimum. The fibres had 7-cell cores but were drawn to different scales, giving them different λ_c but otherwise comparable properties [30]. The minimum attenuation is plotted in Fig. 3 against λ_c on a log-log scale. A straight-line fit is shown and has a slope of 3.07, supporting the predicted inverse cubic dependence in Eq. (6).

The low-loss part of the measured attenuation spectrum of a 7-cell Hollow-core photonic crystal fiber, with a minimum of 700 dB/km at λ_c=550 nm. (left inset) Measured nearfield pattern at the output of this fibre at 550 nm. (points). The minimum attenuation of similar HC-PCFs with various transverse scales, versus the wavelength λ_c of minimum attenuation (broken red line). A straight-line fit to the points, having a slope of 3.07. (right inset) SEM of a representative of these Hollow-core photonic crystal fibers, with λ_c≈1550 nm.

The minimum optical attenuation of ~0.15 dB/km in conventional fibers [33] is determined by fundamental scattering and absorption processes in the high-purity

glass [32, 34], leaving little prospect of much improvement. However, over 99 % of the light in HC-PCFs can propagate in air [27] and avoid these loss mechanisms, making Hollow-core photonic crystal fibers promising candidates as future ultra-low loss telecommunication fibers. Nevertheless the lowest loss reported in Hollow-core photonic crystal fibers is 1.7 dB/km [27], though we have since reduced this to 1.2 dB/km. An understanding of the fundamental limitations to this loss is therefore of great importance. Since only a small fraction of the light propagates in silica, the effect of material nonlinearities is insignificant and the fibers do not suffer from the same limitations on loss as conventional fibers made from solid material alone.

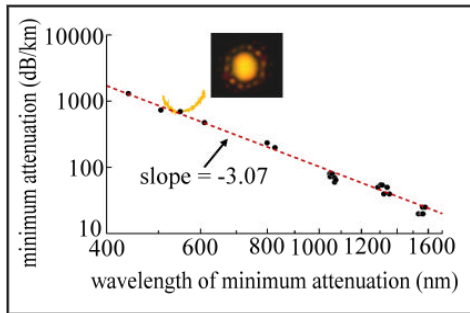


Fig. 3. (solid orange curve)

6. The photonic crystal fiber requirements

These general requirements can be captured by a set of more specific performance parameters as described below.

6.1. Optical Path Length

Longer optical path lengths generally provide improved measurement sensitivity, and this can be achieved with longer fiber lengths, especially in the photonic crystal fiber gyroscope (PCFG) configuration. Table 1 shows a comparison of optical path length between hollow core and conventional fibers.

Table 1

Gives a comparison of optical path length for hollow core and conventional silica core fibers.

Feature	Conventional fiber	Hollow core fiber
Loss (PM fiber) @ 1550 nm	<3 dB/km	<15 dB/km
Loss (PM fiber) @ 1550 nm	<3 dB/km	<2 dB/km
Nonlinearities	Kerr effect limits	Est.>100x better
Coupling	Reflectivity advantage if splicing to other fiber components (IFOG)	Reflectivity advantage if free-space coupling (RFOG)

To support that requirement, the fiber should have:

- low loss per unit length, to satisfy the optical power budget allocation for fiber loss;
- low backscatter, to prevent noise and associated measurement error;
- low nonlinearities, such as the Kerr effect, whereby refractive index dependencies in the light-guiding material due to electric field can cause a non-reciprocal effect in the fiber loop leading to measurement error;

- effective coupling/interfaces, relating to power loss and to interface reflections and crosstalk mechanisms, thereby affecting other system design decisions and overall measurement performance.

6.2. Form Factor

Smaller size is a feature of PCFG when compared to mechanical and ring laser gyroscopes. Table 2 shows a comparison of Form Factor between hollow core and conventional fibers.

Table 2

Gives a comparison of the form factor for hollow core and conventional silica core fibers.

Feature	Conventional fiber	Hollow core fiber
Fiber diameter	Typ. 80 μm clad, 170 μm coating	Development fibers 125 μm clad, 240 μm clad
Fiber bend diameter	Typ. 2–3 inch	<1 inch

To achieve the long optical path length in a small form factor some of the optical fiber features to consider are:

- small fiber glass and coating diameter, to enable many turns of fiber in a limited coil space;
- low bend sensitivity, to enable smaller coil inner diameters without compromising optical power as a result of increased bending loss.

6.3. Stability

Stable performance and low drift are especially critical in high performance gyroscopes. Table 3 shows a comparison of the stability between hollow core and conventional fibers.

Table 3

Gives a comparison of the stability for hollow core and conventional silica core fibers

Feature	Conventional fiber	Hollow core fiber
Thermal stability	Shupe effect limits	Est. >7x better
Polarization maintenance thermal stability	Poor if using stress parts for polarization maintenance	Better than stress part designs
Radiation sensitivity	Poor if using co-doped silica	Est. 50x better
Magnetic sensitivity	Faraday effect limits (less in a PM fiber)	Est. >100x better

Fibers must provide stable performance in a number of areas:

- thermal stability, such that a wide temperature range can be supported and thermal gradients do not cause non-reciprocal index changes (Shupe effect). The polarization maintaining properties of a fiber should also be insensitive to temperature;
- radiation insensitivity, in particular for applications such as space and aircraft navigation/guidance;
- magnetic field insensitivity, as fibers sensitive to this (Faraday effect) may require additional shielding in the gyroscope design.

6.4. Hollow core fiber

Hollow core fiber is based on microstructured fiber design using a photonic bandgap (PBG) cladding composed of silica and air holes surrounding a hollow core for guiding, as shown in Fig. 4 [35]. The photonic bandgap guiding

mechanism is fundamentally different from the traditional total internal reflection guiding principle in conventional fibers.

For fiber gyroscopes, hollow core fibers offer a number of advantages over solid core silica fibers. This technology provides for

- Low nonlinearities. As more than 98 % of the mode is confined in air, not silica, the fibers are less sensitive to nonlinearities such as the Kerr effect.
- Pure silica material, with no co-dopants that can add to fiber environmental sensitivities.
- No Fresnel reflections at open fiber end when free-space coupling in air.
- Polarization maintaining design using form birefringence for low temperature sensitivity.
- Low bend sensitivity of fibers may be bent to very small diameters of less than 1 inch without added losses, thereby enabling smaller form factor designs.

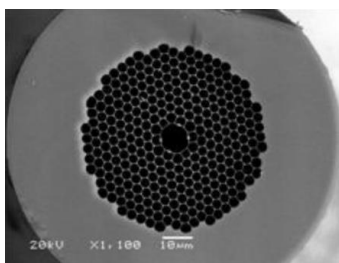


Fig. 4. Hollow core fiber cross section of core and cladding region

It is designed example that may be useful in PCFG designs are shown in Fig. 5, with both fibers designed for transmission near 1550 nm. Fig. 5 (left) shows a polarization maintaining design. The core wall has an asymmetric set of glass enlargements around the core wall that is design features to create a thermally-insensitive form birefringence. Losses for this fiber are near 15 dB/km. Fig. 5 (right) shows a larger core design (more multi-moded) optimized for low loss, with losses for this fiber near 3 dB/km.

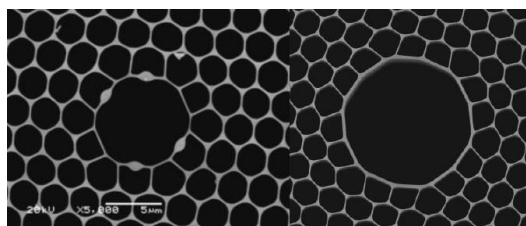


Fig. 5. A polarization maintaining hollow core fiber (left), and a larger core lower loss design (right)

It is anticipated that fiber loss in a hollow core fiber will approach levels achieved by conventional fibers as the technology development continues. The opportunity for continued performance improvements with these fibers will only increase the advantages over conventional fibers.

7. Interferometer based on photonic crystal fibers

The main argument in favor of a replacement optical fiber to another medium, is that the first Sagnac experiments conducted in the hollow pipe and the low pressure air is not

observed effects are manifested in the optical fiber. In this regard, it is evident that the use of such optical media, which on the one hand, would allow optical radiation to channel, and on the other hand did not change to its frequency and phase characteristics. Such environments include photonic crystals with defects. In such environments, the defect is a hollow waveguide. Manufactured photonic crystal fiber has a refractive index of 1.82 at wavelength 500 nm for this fiber type Kagome effective single-mode propagation occurs in a wavelength range from 750 to 1050 nm in diameter mainly 30micro and loss of about 0.7 dB/m [36] see Fig. 6.

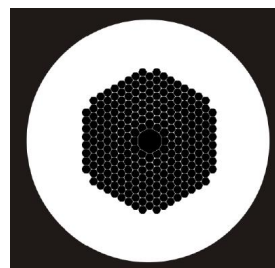


Fig. 6. An example of a photonic crystal fiber with a hollow core diameter of about 30 microns

The collapsed zones in the PCF cause a broadening of the beam when it propagates from the SMF to the PCF [37, 38]. The broadening of the beam combined with the axial symmetry and the modal properties of the PCF are what allow the excitation (and recombination) of modes that have similar azimuthal symmetry [39]. The modes excited in the PCF have different effective indices (or different propagation constants), thus they travel at different speeds. As a result, the modes accumulate a phase difference as they propagate along the PCF. Due to the excitation and recombination of modes in the device, the reflection spectrum is expected to exhibit a series of maxima and minima (interference pattern). When two modes participate in the interference the transmitted or reflected intensity (I) can be expressed as:

$$I = I_1 + I_2 + 2\sqrt{I_1 I_2} \cos(\Delta\Phi) \tag{7}$$

In Equation (7) I_1 and I_2 are, respectively, the intensity of the core mode and the cladding mode and $\Delta\Phi = 2\pi\Delta nL/\lambda$ is the total phase shift. $\Delta n = n_f - n_c$, n_f and n_c being, respectively, the effective refractive index of the core mode and the cladding mode. L is the physical length of the PCF and λ the wavelength of the optical source. The fringe spacing or period (P) of the interference pattern is given by $P = \lambda^2/(\Delta nL)$. The maxima of the interference pattern appear at wavelengths that satisfy the condition $\Delta\Phi = 2m\pi$, with $m = 1, 2, 3...$ This means at wavelengths given by

$$\lambda_m = \Delta n \frac{L}{m} \tag{8}$$

The fringe contrast or visibility (V) of a modal interferometer is an important parameter, particularly when the interferometer is used for sensing applications. Typically, higher visibility is desirable since it leads to larger signal-to-noise ratio and more accurate measurement. The visibility of a two-mode interferometer can be calculated by the well-known expression: $V = (I_{max} - I_{min}) / (I_{max} + I_{min})$, where I_{max}

and I_{\min} are, respectively, the maximum and minimum values of I given in Equation (7). According to the definition and Equation (7) V can be expressed as [40]:

$$V = \frac{2\sqrt{k}}{(1+k)}, \tag{9}$$

where $k=I_1/I_2$.

Many research groups prefer fringe contrast (expressed in dB) instead of visibility. The fringe contrast (FC) is defined here as $FC=-10\log(1-V)$. In Fig. 5 we show the dependence of the fringe contrast on k along with the theoretical interference pattern of device with $L=10$ mm for two values of k . It can be noted that the fringe contrast increases as k approaches to 6, i. e., when the two modes that participate in the interference have equal intensities. Fig. 7. Fringe contrast in a mode interferometer as a function of k or the intensity of the cladding mode to that of the core mode ratio. Fig. 8 shows the theoretical reflection of spectrum in the case of $k=0.4$ (dotted line) and $k=0.96$ (solid line).

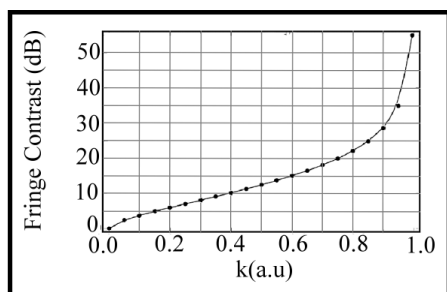


Fig. 7. Fringe contrast in a mode interferometer

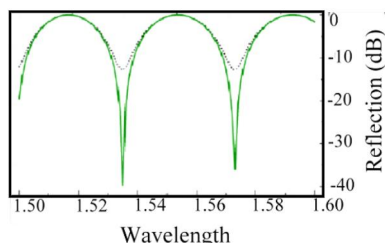


Fig. 8. Theoretical reflection of spectrum

The physical mechanism for the waveguide propagation of radiation in photonic fibers is not associated with the phenomenon of total internal and with the presence of the photonic band gap in the transmission spectrum of the fiber cladding. Waveguides of this type are promising for the creation of gas sensors, spectral elements, as well as laser-cooled atoms management. Experimental studies have shown that in some cases [41]. Relatively high loss optical fibers with core air owing to scattering of light by irregularities of the glass surface due to the capillary waves frozen. Solution to reduce optical loss photonic fibers requires further fundamental research, however, we can already use small pieces of photonic fibers in special measuring instruments, which include the FOG. Photonic crystal fiber is a two-dimensional photonic crystal structure based on the song “quartz glass-to-air” formed in the shell.

8. Propagation of optical radiation in photonic crystal defect

In [42] were considered in detail the conditions of formation of photonic crystal fibers and spread them in the optical radiation. Experimental studies of PCF were conducted in a number of studies, for example, [43]. Photonic band gaps arising in the transmission spectrum of a two-dimensional periodic cladding, provides a high reflection coefficient for radiation propagating along the hollow core, realizing mode waveguide propagation. In [43] the results of an experimental determination of the optical emission intensity distribution in the cross-sectional center of the defect and the results of numerical calculation of the distribution of power density in cross-section. These results are shown in Fig. 9

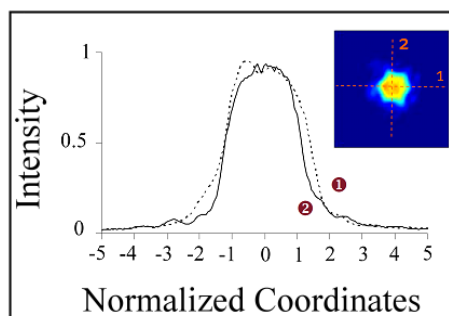


Fig. 9. Distribution of the output power with a hollow core PCF

To date, published studies on the conditions of use of PCF for transmitting optical information signals in telecommunication systems, however, the use of PCF in optical interferometers have only begun to explore, for precision measurements of some physical quantities. In [44] the results of measurement of voltage using a cylindrical PCF, which is formed by the interferometer. To describe the operation of a fiber gyroscope based on PCF must use the description of the optical waves propagating along the two-dimensional photonic crystal defect [45]. To implement the necessary PCF fiber gyroscope with a minimum loss of less than 1 dB/km, that extends single-mode radiation. These fibers include, for example, commercially available PCF – HC19-1550 (0,03 dB/km) or LMA-25 (1,5 dB/km) operating at 1550 nm. The low level of absorption in these fibers allows you to create on their basis multiturn ring interferometer, which implements the Sagnac effect. The main technical challenge in applying PCF is the junction of the individual elements of the PCF, Here are some distinctive features of the assembly fiber interferometer.

10. Conclusion

Photonic crystal fiber gyroscopes are a kind of optics gyroscopes that present a diversity of new and improved features beyond what conventional optical fiber gyroscopes can offer. Due to their unique geometric structure, photonic crystal fibers present special properties and capabilities that lead to an outstanding potential for sensing applications. The paper discusses the benefits of using hollow core photonic crystal fiber, 1550 nm,

Ø10 µm instead of the conventional fibers in optical gyroscope. They can provide dielectric isolation between the sensor and the interrogation system in the presence of very high electromagnetic fields.

References

1. Knight, J. C. All-silica single-mode optical fiber with photonic crystal cladding [Text] / J. C. Knight, T. A. Birks, P. S. J. Russell, D. M. Atkin // Optics Letters. – 1996. – Vol. 21, Issue 19. – P. 1547–1549. doi: 10.1364/ol.21.001547
2. Chau, Y.-F. A comparative study of high birefringence and low confinement loss photonic crystal fiber employing elliptical air holes in fiber cladding with tetragonal lattice [Text] / Y.-F. Chau, C.-Y. Liu, H.-H. Yeh, D. P. Tsai // Progress In Electromagnetics Research B. – 2010. – Vol. 22. – P. 39–52. doi: 10.2528/pierb10042405
3. Ortigosa-Blanch, A. Highly birefringent photonic crystal fibers [Text] / A. Ortigosa-Blanch, J. C. Knight, W. J. Wadsworth, J. Arriaga, B. J. Mangan, T. A. Birks, P. S. J. Russell // Optics Letters. – 2000. – Vol. 25, Issue 18. – P. 1325–1327. doi: 10.1364/ol.25.001325
4. Chen, D. Ultrahigh birefringent photonic crystal fiber with ultralow confinement loss [Text] / D. Chen, L. Shen // IEEE Photonics Technology Letters. – 2007. – Vol. 19. – P. 185–187. doi: 10.1109/lpt.2006.890040
5. Agrawal, A. Golden spiral photonic crystal fiber: Polarization and dispersion properties [Text] / A. Agrawal, N. Kejalakshmy, J. Chen, B. M. A. Rahman, K. T. V. Grattan // Optics Letters. – 2008. – Vol. 33, Issue 22. – P. 2716–2718. doi: 10.1364/ol.33.002716
6. Yang, S. Theoretical study and experimental fabrication of high negative dispersion photonic crystal fiber with large area mode field [Text] / S. Yang, Y. Zhang, X. Peng, Y. Lu, S. Xie, J. Li, W. Chen, Z. Jiang, J. Peng, H. Li // Optics Express. – 2006. – Vol. 14, Issue 7. – P. 3015–3023. doi: 10.1364/oe.14.003015
7. Ju, J. Design of single-polarization single mode photonic crystal fibers [Text] / J. Ju, W. Jin, M. S. Demokan // J. Lightwave Technol. – 2001. – Vol. 24. – P. 825–830.
8. Kubota, H. Absolutely single polarization photonic crystal fiber [Text] / H. Kubota, S. Kawanishi, S. Koyanagi, M. Tanaka, S. Yamaguchi // IEEE Photonics Technology Letters. – 2004. – Vol. 16, Issue 1. – P. 182–184. doi: 10.1109/lpt.2003.819415
9. Knight, J. C. Nonlinear waveguide optics and photonic crystal fibers [Text] / J. C. Knight, D. V. Skryabin // Optics Express. – 2007. – Vol. 15. – P. 15365–15376. doi: 10.1364/oe.15.015365
10. Mortensen, N. A. Improved large-mode-area endlessly single mode photonic crystal fibers [Text] / N. A. Mortensen, M. D. Nielsen, J. R. Folkenberg, A. Petersson, and H. R. Simonsen // Optics Letters. – 2003. – Vol. 28, Issue 6. – P. 393–395. doi: 10.1364/ol.28.000393
11. Folkenberg, J. Polarization maintaining large mode area photonic crystal fiber [Text] / J. Folkenberg, M. Nielsen, N. Mortensen, C. Jakobsen, H. Simonsen // Optics Express. – 2004. – Vol. 12, Issue 5. – P. 956–960. doi: 10.1364/opex.12.000956
12. Dobb, H. Temperature-insensitive long period grating sensors in photonic crystal fibre [Text] / H. Dobb, K. Kalli, D. J. Webb // Electronics Letters. – 2004. – Vol. 40, Issue 11. – P. 657–658. doi: 10.1049/el:20040433
13. Dong, X. Temperature-insensitive strain sensor with polarization-maintaining photonic crystal fiber based on Sagnac interferometer [Text] / X. Dong, H. Y. Tam // Applied Physics Letters. – 2007. – Vol. 90, Issue 15. – P. 151113. doi: 10.1063/1.2722058
14. Wadsworth, W. J. Yb³⁺-doped photonic crystal fibre laser [Text] / W. J. Wadsworth, J. C. Knight, W. H. Reewes, P. S. J. Russell, J. Arriaga // Electronics Letters. – 2000. – Vol. 36, Issue 17. – P. 1452–1453. doi: 10.1049/el:20000942
15. Chen, D. Stable multi-wavelength erbium-doped fiber laser based on photonic crystal fiber Sagnac loop filter [Text] / D. Chen // Laser Physics Letters. – 2007. – Vol. 4, Issue 6. – P. 437–439. doi: 10.1002/lapl.200710003
16. Broderick, N. G. R. Nonlinearity in holey optical fibers: Measurement and future opportunities [Text] / N. G. R. Broderick, T. M. Monro, P. J. Bennett, D. J. Richardson // Optics Letters. – 1999. – Vol. 24, Issue 20. – P. 1395–1397. doi: 10.1364/ol.24.001395
17. Dudley, J. M. Ten years of nonlinear optics in photonic crystal fibre [Text] / J. M. Dudley, J. R. Taylor // Nature Photonics. – 2009. – Vol. 3, Issue 2. – P. 85–90. doi: 10.1038/nphoton.2008.285
18. Overview of Fiber Optic Sensors [Electronic resource] / Available at: http://www.bluer.com/images/Overview_of_FOS2.pdf (Last accessed: 8.02.2012).
19. Yablonovitch, E. Photonic Band Structure: The Face-Centered-Cubic Case Employing Nonspherical Atoms [Text] / E. Yablonovitch, T. J. Gmitter, K. M. Leung // Physical Review Letters. – 1991. – Vol. 67, Issue 17. – P. 2295–2298. doi: 10.1103/physrevlett.67.2295
20. Birks, T. A. Full 2-D photonic bandgaps in silica/air structures [Text] / T. A. Birks, P. J. Roberts, P. S. J. Russell, D. M. Atkin, T. J. Shepherd // Electronics Letters. – 1995. – Vol. 31, Issue 22. – P. 1941–1943. doi: 10.1049/el:19951306
21. Knight, J. C. All-silica single-mode optical fiber with photonic crystal cladding [Text] / J. C. Knight, T. A. Birks, P. S. J. Russell, D. M. Atkin // Optics Letters. – 1996. – Vol. 21, Issue 19. – P. 1547–1549. doi: 10.1364/ol.21.001547
22. Ho, H. L. Optimizing microstructured optical fibers for evanescent wave gas sensing [Text] / H. L. Ho, Y. L. Hoo, W. Jin, J. Ju, D. N. Wang, R. S. Windeler, Q. Li // Sensors and Actuators B. – 2007. – Vol. 122, Issue 1. – P. 289–294. doi: 10.1016/j.snb.2006.05.036
23. Bock, W. J. A photonic crystal fiber sensor for pressure measurements [Text] / W. J. Bock, J. Chen, T. Eftimov, W. Urbanczyk // IEEE Transactions on Instrumentation and Measurement. – 2006. – Vol. 55, Issue 4. – P. 1119–1123. doi: 10.1109/tim.2006.876591
24. Andronova, I. A. Physical problems of fibergiroscope based on the Sagnac effect [Text] / I. A. Andronova, G. B. Malykin // Physics-Uspokhi. – 2002. – Vol. 45, Issue 8. – P. 793–817. doi: 10.1070/pu2002v045n08abeh001073

25. Shinde, Y. S. Dynamic pressure sensing study using photonic crystal fiber: application to tsunami sensing [Text] / Y. S. Shinde, H. K. Gahir // *IEEE Photonics Technology Letters*. – 2008. – Vol. 20, Issue 4. – P. 279–281. doi: 10.1109/lpt.2007.913741
26. Russell, P. Photonic crystal fibers [Text] / P. Russell // *Science*. – 2003. – Vol. 299, Issue 5605. – P. 358–362. doi: 10.1126/science.1079280
27. Mangan, B. J. Low loss (1.7 dB/km) hollow core photonic bandgap fiber [Text] / B. J. Mangan, L. Farr, A. Langford, P. J. Roberts, D. P. Williams, F. Couny, M. Lawman, M. Mason, S. Coupland, R. Flea, H. Sabert, T. A. Birks, J. C. Knight and P. Russell // in *Proc. Opt. Fiber. Commun.* – 2004. paper PDP24.
28. Ravi Kanth Kumar, V. V. Extruded soft glass photonic crystal fiber for ultrabroad supercontinuum generation [Text] / V. V. Ravi Kanth Kumar, A. George, W. Reeves, J. Knight, P. Russell, F. Omenetto, A. Taylor // *Opt. Express*. – 2002. – Vol. 10, Issue 25. – P. 1520. doi: 10.1364/oe.10.001520
29. Ebendorff-Heidepriem, H. Suspended nanowires: fabrication, design and characterization of fibers with nanoscale cores [Text] / H. Ebendorff-Heidepriem, S. C. Warren-Smith, T. M. Monro // *Opt. Express*. – 2009. – Vol. 17, Issue 4. – P. 2646. doi: 10.1364/oe.17.002646
30. Cregan, R. F. Singlemode photonic band gap guidance of light in air [Text] / R. F. Cregan, B. J. Mangan, J. C. Knight, T. A. Birks, P. Russell, P. J. Roberts, D. C. Allan // *Science*. – 1999. – Vol. 285, Issue 5433. – P. 1537–1539. doi: 10.1126/science.285.5433.1537
31. Payne, F. P. A theoretical analysis of scattering loss from planar optical waveguides [Text] / F. P. Payne, J. P. R. Lacey // *Optical and Quantum Electronics*. – 1994. – Vol. 26, Issue 10. – P. 977–986. doi: 10.1007/bf00708339
32. Miya, T. Ultimate low-loss single-mode fibre at 1.55 μm [Text] / T. Miya, Y. Terunuma, T. Hosaka, T. Miyashita // *Electronics Letters*. – 1979. – Vol. 15, Issue 4. – P. 106–108. doi: 10.1049/el:19790077
33. Nagayama, K. Ultra-low-loss (0.1484 dB/km) pure silica core fibre and extension of transmission distance [Text] / K. Nagayama, M. Kakui, M. Matsui, I. Saitoh and Y. Chigusa // *Electronics Letters*. – 2002. – Vol. 38, Issue 20. – P. 1168–1169. doi: 10.1049/el:20020824
34. Ohashi, M. Optical loss property of silica-based single-mode fibers [Text] / M. Ohashi, K. Shiraki, K. Tajima // *Journal of Lightwave Technology*. – 1992. – Vol. 10, Issue 5. – P. 539–543. doi: 10.1109/50.136085
35. Sanders, G. A. Hollow Core Fiber Optic Ring Resonator for Rotation Sensing [Text] / G. A. Sanders, L. K. Strandjord, T. Qiu. – *Optical Fiber Sensors*. – OSA Technical Digest (Optical Society of America), 2006. doi: 10.1364/ofs.2006.me6
36. Jiang, X. Single-mode hollow-core photonic crystal fiber made from sift glass [Text] / X. Jiang, T. G. Euser, F. Abdolvand, F. Babic, F. Tani, N. Y. Joly, J. C. Travers, P. St. J. Russell // *Optics express*. – 2011. – Vol. 19, Issue 16. – P. 15438–15444. doi: 10.1364/oe.19.015438
37. Jha, R. Ultrastable in reflection photonic crystal fiber modal interferometer for accurate refractive index sensing [Text] / R. Jha, J. Villatoro, G. Badenes // *Applied Physics Letters*. – 2008. – Vol. 93, Issue 19. – P. 191106:1–191106:3. doi: 10.1063/1.3025576
38. Jha, R. Refractometry based on a photonic crystal fiber interferometer [Text] / R. Jha, J. Villatoro, G. Badenes, V. Pruneri // *Optics Letters*. – 2009. – Vol. 34, Issue 5. – P. 617–619. doi: 10.1364/ol.34.000617
39. Cárdenas-Sevilla, G. A. Photonic crystal fiber sensor array based on modes overlapping [Text] / G. A. Cárdenas-Sevilla, V. Finazzi, J. Villatoro, V. Pruneri // *Optics Express*. – 2011. – Vol. 19, Issue 8. – P. 7596–7602. doi: 10.1364/oe.19.007596
40. Zhang, Y. Fringe visibility enhanced extrinsic Fabry-Perot interferometer using a graded index fiber collimator [Text] / Y. Zhang, Y. Li, T. Wei, X. Lan, Y. Huang, G. Chen, H. Xiao // *IEEE Photonics Journal*. – 2010. – Vol. 2, Issue 3. – P. 469–481. doi: 10.1109/jphot.2010.2049833
41. Tuchin, V. V. Sensornye svoystva fotonno-kristallicheskogo volnovoda s poloj serdcevinov [Text] / V. V. Tuchin, Ju. S. Skibina, V. I. Beloglazov et. al. // *Pis'ma v ZhTF*. – 2008. – Vol. 34, Issue 15. – P. 63–69.
42. Russell, P. J. Photonic-Cristal Fibers [Text] / P. J. Russell // *Journal of Lightwave technology*. – 2006. – Vol. 24, Issue 12. – P. 4729–4749.
43. Fedotov, A. B. Volnovodnye svoystva i spektr sobstvennyh mod polyh fotonno-kristallicheskih volokon [Text] / A. B. Fedotov, S. O. Kononov, O. A. Koletovatova et. al. // *Kvantovaja jelektronika*. – 2003. – Vol. 33, Issue 3. – P. 271–274.
44. Chen, W. Ring-core photonic crystal fiber interferometer for strain measurement [Text] / W. Chen, S. Lou, L. Wang, S. Jian // *Optical Engineering*. – 2010. – Vol. 49, Issue 9. – P. 094402. doi: 10.1117/1.3488045
45. Mogilevtsev, D. Localized Function Method for Modelling Defect Modes in 2-d Photonic Crystals [Text] / D. Mogilevtsev, T. A. Birks, P. J. Russell // *Journal of lightwave technology*. – 1999. – Vol. 17, Issue 11. – P. 2078–2081. doi: 10.1109/50.802997